Cellular Physiology and Biochemistry

Cell Physiol Biochem 2022;56:254-269
DOI: 10.33594/000000531
Published online: 7 June 2022
Accepted: 25 May 2022







**Original Paper**

# Supporting Cells of the Human Olfactory Epithelium Co-Express the Lipid Scramblase TMEM16F and ACE2 and May Cause Smell Loss by SARS-CoV-2 Spike-Induced Syncytia

Andres Hernandez-Clavijo[a] Kevin Y. Gonzalez-Velandia[a] Uday Rangaswamy[a] Giorgia Guarneri[a] Paolo Boscolo-Rizzo[b] Margherita Tofanelli[b] Nicoletta Gardenal[b] Remo Sanges[a] Michele Dibattista[c] Giancarlo Tirelli[b] Anna Menini[a]

[a]Neuroscience Area, SISSA, Scuola Internazionale Superiore di Studi Avanzati, Trieste, Italy, [b]Department of Medical, Surgical and Health Sciences, Section of Otolaryngology, University of Trieste, Trieste, Italy, [c]Department of Basic Medical Sciences, Neuroscience and Sensory Organs, University of Bari A. Moro, Bari, Italy

**Key Words**
Sustentacular cells • ANO6 • Human olfaction • Scramblase

**Abstract**
***Background/Aims:*** Quantitative and qualitative alterations in the sense of smell are well established symptoms of COVID-19. Some reports have shown that non-neuronal supporting (also named sustentacular) cells of the human olfactory epithelium co-express ACE2 and TMPRSS2 necessary for SARS-CoV-2 infection. In COVID-19, syncytia were found in many tissues but were not investigated in the olfactory epithelium. Some studies have shown that syncytia in some tissues are formed when SARS-CoV-2 Spike expressed at the surface of an infected cell binds to ACE2 on another cell, followed by activation of the scramblase TMEM16F (also named ANO6) which exposes phosphatidylserine to the external side of the membrane. Furthermore, niclosamide, an approved antihelminthic drug, inhibits Spike-induced syncytia by blocking TMEM16F activity. The aim of this study was to investigate if proteins involved in Spike-induced syncytia formation, i.e., ACE2 and TMEM16F, are expressed in the human olfactory epithelium. ***Methods:*** We analysed a publicly available single-cell RNA-seq dataset from human nasal epithelium and performed immunohistochemistry in human nasal tissues from biopsies. ***Results:*** We found that ACE2 and TMEM16F are co-expressed both at RNA

A. Hernandez-Clavijo and K. Y. Gonzalez-Velandia contributed equally to this work.

Anna Menini
and Michele Dibattista

SISSA, Neuroscience Area, Via Bonomea 265, Trieste (Italy)
Tel. +39-0403787706, E-Mail anna.menini@sissa.it

Department of Basic Medical Sciences, Neuroscience and Sensory Organs,
University of Bari A. Moro, Piazza Giulio Cesare 11, Bari (Italy)
E-Mail michele.dibattista@uniba.it

and protein levels in non-neuronal supporting cells of the human olfactory epithelium. ***Conclusion:*** Our results provide the first evidence that TMEM16F is expressed in human olfactory supporting cells and indicate that syncytia formation, that could be blocked by niclosamide, is one of the pathogenic mechanisms worth investigating in COVID-19 smell loss.



## Introduction

The toll of the coronavirus disease 2019 (COVID-19) has been very high over the past two years. Since the beginning of the pandemic, various efforts have been made to identify the most common symptoms and among these the loss of chemosensory abilities has been identified as a predominant and frequently long-lasting symptom of this disease [1–6]. Although impairment in the sense of smell is common to other infectious respiratory diseases [7, 8], it was surprising and unprecedented that both its onset and evolution were unrelated to other flu-like symptoms (or sometimes to any other symptom, as often smell loss was the only symptom) including nasal obstruction [5, 9]. Indeed, an alteration in the sense of smell is used as part of routine screening for COVID-19 [10, 11].

COVID-19 disease is caused by the severe acute respiratory syndrome coronavirus strain 2 (SARS-CoV-2), a positive-sense single strand RNA virus. The genome is composed of about 30 Kbp RNA and encodes for sixteen non-structural proteins, four structural proteins and eight accessory proteins [12]. Coronaviruses take their name from their electron micrographs showing several petal-shaped projections, called Spikes, that are reminiscent of the solar corona [13]. Spikes are glycoproteins protruding from the viral envelop and bind to their canonical human receptor Angiotensin Converting Enzyme 2 (ACE2) [14, 15]. The fast pace of the research on the pathogenic mechanism of action of SARS-CoV-2 has given several clues on what happens when the virus enters in contact with host cells. The binding of the Spike protein with ACE2 determines virus-cell adhesion thus unleashing its fusion machinery to infiltrate the cell [16, 17]. The Spike protein contains consensus sequences that could be further modified by host proteases furin and TMPRSS2. The furin is important to cleave the spike protein priming it for cell entry, then TMPRSS2 facilitates it by allowing a non-endosomal early entry of the virus [14, 18, 19].

It has been recently discovered that the SARS-CoV-2 Spike protein can cause fusion between cells and syncytia formation [17, 20–27] and that a mutation in its receptor binding site impaired cell-to-cell fusion and syncytia formation [28]. For example, multinucleated pneumocytes were found in the lung of patients deceased for COVID-19 [20, 29, 30]. Recently, the TMEM16F protein, also named ANO6, has been shown to be involved in syncytia formation. TMEM16F is a calcium-activated scramblase and ion channel [31–34] that is responsible for exposing phosphatidylserine from the cytofacial to the exofacial leaflet of the plasma membrane and can therefore act as signalling molecule for cell-to-cell fusion [25, 30, 35, 36]. In addition, the same mechanism has been proposed to enhance platelet pro-coagulant activity [22].

As the molecular mechanisms underlying the olfactory dysfunction in COVID-19 are still largely unknown, we asked whether SARS-CoV-2 Spike protein could trigger syncytia formation in the human olfactory epithelium. The olfactory epithelium is a pseudo-stratified epithelium consisting of different cell types (Fig. 1A) [37–39]. The functional units expressing odorant receptors are the bipolar olfactory sensory neurons which bear several apical cilia protruding in the nasal cavity and contain the molecular components for odorant transduction. These neurons are surrounded, basically enwrapped by supporting cells, also named sustentacular cells, a columnar-like type of cells. Stem cells (horizontal and globose basal cells) are located at the base of the olfactory epithelium [39–41]. These basal cells are pluripotent and replace both supporting cells and olfactory sensory neurons constituting a neurogenic niche able to regenerate the human olfactory epithelium [42]. Previous work has shown that supporting cells and basal cells, but not olfactory sensory neurons, express both ACE2 and TMPRSS2 that allow SARS-CoV-2 entry into these cells [43–45].

To investigate if ACE2 and TMEM16F, the molecular components necessary for syncytia formation, are co-expressed in cells of the olfactory epithelium, we analysed a single-cell RNA-seq (scRNA-seq) dataset from human nasal epithelium [42] and performed immunohistochemistry in human nasal tissues from biopsies. We found that ACE2 and TMEM16F are co-expressed both at RNA and protein levels in non-neuronal supporting cells. We propose that one of the pathogenic mechanisms behind smell loss could be syncytia formation of supporting cells initiated by Spike binding to ACE2 and mediated by TMEM16F.

## Materials and Methods

*Single-cell RNA sequencing data analysis*

The single-cell RNA-seq dataset was downloaded from NCBI GEO: GSE139522 and was related to the study by Durante et al. [42]. The dataset consists of single cell 3' RNAseq of the olfactory epithelium from 2 individuals and respiratory epithelium from other 2 individuals. Individuals involved in this study were aged between 41 and 52 years. Tissue for sequencing was obtained while undergoing transnasal endoscopic surgery. 10X Genomics Chromium platform and Illumina Nextseq 500 technology was used for sequencing. The data was analysed in R version 4.1.2 using the Seurat R package version 4.1.0 [46–48], a widely used toolkit for quality control, analysis and exploration of single cell RNA sequencing data. The procedures described in Durante et al. [42] with minimal modifications were used for analysing this dataset.

The raw gene-barcode matrix of all 4 patients were loaded into R using Read10X() function of Seurat. A Seurat object was created for each individual data using the CreateSeuratObject() function. PercentageFeatureSet() function was used to calculate the percentage of mitochondrial gene counts for each Seurat object. Cells that had UMI > 400, between 100-8000 expressed genes and mitochondrial content less than 10% were defined as high-quality cells and considered for downstream analysis. This filtering resulted in a total of 29628 cells across all 4 Seurat objects.

The filtered Seurat objects were merged using the merge() function provided by the Seurat package. Each individual data was separated using the SplitObject() function. The raw UMI count of the genes within each cell was normalized by the total number of UMI counts per cell, scaled to $10^4$ and natural log transformed using the NormalizeData() function for each dataset. The top 5000 variable genes were identified for each dataset using FindVariableFeatures() function, with variance stabilizing transformation (vst) as the selection method. This was followed by identifying the anchor genes using the FindIntegrationAnchors() function with default parameters. It returned the top 5000 variable genes shared across the 4 datasets. The datasets were integrated into a single Seurat object using the IntegrateData() function with default parameters.

The integrated data was scaled and reduced to 30 principal components (PCs) using the ScaleData() and RunPCA() function of Seurat. These PCs were passed as input to the RunUMAP() function. Clustering was done using FindNeighbors() and FindClusters() functions using the 30 PCs and a resolution parameter of 0.5 which resulted in 27 Louvain clusters. The clustering results were visualized in a two-dimensional UMAP representation produced using the DimPlot() function. The clusters were annotated based on the expression of the canonical marker genes for different cell types as mentioned in Durante et al. The AddModuleScore() and FeaturePlot() functions were used to visualize the expression of the canonical marker genes to annotate the clusters. Multiple clusters were annotated as one cell type when the expression of the marker genes for that cell type was highly expressed in multiple clusters. When the expression of marker genes for more than one cell type was found to be highly expressed in a single cluster, that cluster was annotated to contain multiple cell types. By doing so, 27 clusters were further reduced to 21 clusters. The following cell type pairs were identified within the same cluster: olfactory and respiratory HBCs (cluster 0), fibroblasts and stromal cells (cluster 1), macrophages and dendritic cells (cluster 11), mature and immature neurons (cluster 15). On the contrary, the following cell types were identified in more than one cluster: supporting cells (also named sustentacular cells cluster 3 and 10), pericytes (cluster 4 and 6), bowman's glands (cluster 12, 16 and 17), plasma cells (cluster 13 and 19) and olfactory HBCs/respiratory HBCs (cluster 0 and 26). The number of cells present in each cluster and cell type is contained in Supplementary Table 1 and 2. Supplementary Fig. S1 shows the co-expression of *TMEM16F*, *ACE2* and *TMPRSS2* in the various cell types (for all supplementary material see www.cellphysiolbiochem.com).

*Human nasal tissue*

Samples from human nasal tissue were obtained at the Section of Otolaryngology of the Department of Medical, Surgical and Health Sciences, University of Trieste, Trieste, Italy, with the written informed consent of each patient for participation in this study, which was approved by the Ethics Committee on Clinical Investigation of the University of Trieste (nr 232/2016 and 110/2021).

Biopsies and nasal brushing were performed in the operating room from patients under general anaesthesia at the end of the scheduled endoscopic sinonasal surgery. Two-three biopsy specimens were obtained from one nostril from the superior septum within the olfactory cleft and adjacent to the middle turbinate using a sickle knife and Blakesley forceps or cupped forceps. Samples were obtained from 8 patients (6 males and 2 females, age between 24 and 75 years). Both olfactory and respiratory epithelium were found in 2 biopsies, only olfactory epithelium in 2 biopsies, and only respiratory epithelium in 4 biopsies. Once collected, specimens were immediately fixed in paraformaldehyde (PFA) at 4% in PBS pH 7.4 for 4 to 10 hours at 4 °C. After fixation, the tissue was kept in PBS pH 7.4 at 4 °C, typically from 2 to 24 hours. Nasal brushings were performed with FLOQSwabs® (COPAN, Italy) swab sampling brush consisting of a molded plastic shaft and a tip coated with perpendicular short Nylon® fibers. The swab was gently moved back and forward and rotated in the olfactory cleft of the nostril opposite the one where the biopsy was taken. After nasal brushing, the swab tip was immersed in PFA at 4% in PBS pH 7.4 for 2 hours for cell fixation and then was kept in PBS pH 7.4 at 4 °C, typically from 2 to 24 hours. Although nasal brushings were taken from the olfactory cleft, we could not observe cells from the olfactory epithelium but only cells from the respiratory epithelium.

*Immunohistochemistry and Immunocytochemistry*

For cryoprotection of biopsies, the tissue was equilibrated overnight in 30% (w/v) sucrose in PBS at 4 °C. Then, the tissue was embedded in cryostat embedding medium (BioOptica) and immediately frozen at −80 °C. 16 µm sections were cut on a cryostat and mounted on Superfrost Plus Adhesion Microscope Slides (ThermoFisher Scientific). Sections were air-dried for 3 hours and used the same day or stored at -20 °C for later use. Cryostat embedding medium was removed from the tissue by incubating the slices in PBS for 15 minutes. The tissue was treated for 15 minutes with 0.5 % (w/v) sodium dodecyl sulfate (SDS) in PBS for antigen retrieval, then washed and incubated in blocking solution (5% normal donkey serum, 0.2% Triton X-100 in PBS) for 90 minutes and finally incubated overnight at 4 °C with the primary antibodies diluted in blocking solution. In the following day, the unbound primary antibodies were removed with PBS washes, then sections were incubated with Alexa Fluor conjugated secondary antibodies (1:500 dilution) in TPBS (0.2% Tween 20 in PBS) for 2 hours at room temperature, washed and mounted with Vectashield (Vector Laboratories) or FluoromontG (ThermoFisher). DAPI (5 mg/ml) was added to the solution containing secondary antibody to stain the nuclei. For nasal brushings, the tip of the swab was transferred into a 2 ml tube and treated for 10 minutes with 0.5 % (w/v) SDS in PBS for antigen retrieval, then the same procedure used for tissue slices was followed until washout of the secondary antibody. Cells were then detached from the swab by gentle agitation and by passing the swab through a 200 µl micropipette tip with the extreme end removed as in Scudieri et al. (2020) [49]. Cells were collected and plated in a µ-Slide 8 Well Grid-500 (Ibidi, Germany) and observed under confocal microscopy Nikon A1R (Nikon, Japan). During immunocytochemical analysis from nasal brushings, we observed several respiratory cells but we did not detect any olfactory sensory neuron.

The following primary antibodies (dilution; catalogue number, company) were used: polyclonal goat anti-OMP (1:1000; 019-22291, Wako), monoclonal mouse anti-β Tubulin III (TUJ1) (1:200; 801202, BioLegend), monoclonal mouse anti-β Tubulin IV (BT4) (1:1000; T7941, Sigma), polyclonal rabbit anti-ERMN (1:200; NBP1-84802, Novus), polyclonal rabbit anti-KERATIN 5 (K5) (1:200; 905501, BioLegend), polyclonal goat anti-ACE2 (1:200; PA5-47488, Invitrogen), polyclonal rabbit anti-ACE2 (1:200; ab15348, Abcam), polyclonal rabbit anti-TMEM16F (1:200; provided by Lily Jan University of California, San Francisco, CA, USA; [50]).The following secondary antibodies were used: donkey anti-rabbit Alexa Fluor Plus 594 (1:500; A32754, Life Technologies), donkey anti-rabbit Alexa Fluor 488 (1:500; A21206, Life Technologies), donkey anti-goat Alexa Fluor 488 Plus (1:500; A32814, Life Technologies), donkey anti-mouse Alexa Fluor 594 (1:500, A-21203, Life Technologies), donkey anti-mouse Alexa Fluor 488 (1:500, A32766, Life Technologies). Control experiments, excluding primary antibodies, were performed for each immunolocalization and shown in Supplementary Figure S2.

Immunostaining for human tissue was performed on all olfactory and respiratory epithelia available to confirm findings. We performed at least 2 independent human tissue replicates for each antibody tested. All attempts at replication were successful.

*Image acquisition*

Z-stack images were acquired using NIS-Elements Nikon software at 1024 ×1024 pixels resolution of each single image and analyzed with ImageJ software (National Institute of Health, USA). Max projections of Z-stacks or individual images within the stacks were used to display results. Figure assembly was performed on ImageJ (National Institutes of Health) using ScientiFig plugin [51]. No image modification was performed other than brightness and contrast adjust.

## Results

In the hunt for a possible pathophysiological mechanism for SARS-CoV-2 induced smell loss, we sought to investigate whether TMEM16F, a calcium-dependent ion channel and scramblase, recently involved in SARS-CoV-2 spike-induced syncytia, is expressed in the human nasal tissues and whether its expression pattern resembles that of ACE2. We reasoned that if ACE2 and TMEM16F are co-expressed in the same cell type, then it may have the molecular components necessary to trigger syncytia formation.

*Main cell types in the human olfactory and respiratory epithelium*

By taking advantage of the available single-cell RNA sequencing (scRNA-seq) dataset of the human olfactory and respiratory epithelium of Durante et al. [42], we performed a standard analysis using uniform manifold approximation and projection (UMAP) and identified clusters of several cell types (Fig. 1B). Cell types included olfactory sensory neurons, olfactory supporting cells and basal cells for the olfactory epithelium, while for the respiratory epithelium cell types included respiratory ciliated cells, secretory cells and basal cells. By immunohistochemistry, we used specific markers to identify some of these cells in biopsies of human nasal tissues obtained from patients undergoing endoscopic nasal surgery. For the respiratory epithelium, we used an antibody against β-tubulin IV (BT4), a marker of the cilia of respiratory ciliated cells [52]. For the olfactory epithelium, we used β-tubulin III (TUJ1) to stain neurons, olfactory marker protein (OMP) to identify mature olfactory sensory neurons, keratin 5 (K5) for horizontal basal cells [52, 53], and ERMN for supporting cells [44, 54].

Fig. 1C shows the boundary between the olfactory and the respiratory epithelium with mature olfactory sensory neurons marked by OMP (red) and the cilia of respiratory ciliated cells stained by β-tubulin IV (BT4, green). To distinguish between zones of olfactory and respiratory epithelium, we also visualized neurons using TUJ1 (Fig. 1D-E). The transition zone between the two epithelia showed the passage from the olfactory neuroepithelium to the neuron-less respiratory epithelium. Basal cells were identified by keratin 5 and showed a pearl necklace-like staining pattern not only at the base of the olfactory but also of the respiratory epithelium (Fig. 1D). To visualize supporting cells, we used ERMN a marker which labels the apical part of supporting cells. Fig. 1E confirmed that ERMN apical expression pattern did not co-localize with that of the neuronal marker TUJ1, indicating that we could indeed use ERMN to exclusively visualize olfactory supporting cells.

*ACE2 transcript and protein expression*

As ACE2 is relevant for SARS-CoV-2 Spike binding, we first identified which cells express *ACE2* transcript. In our UMAP analysis we could identify cells expressing *ACE2* in specific populations of the nasal tissue (Fig. 2A-B). We observed *ACE2* expression in several olfactory supporting cells, horizontal basal cells, secretory and ciliated respiratory cells, whereas we could not identify *ACE2* expression in olfactory sensory neurons in the scRNA-seq data. We then evaluated the expression and localization of the ACE2 protein in the human nasal cavity

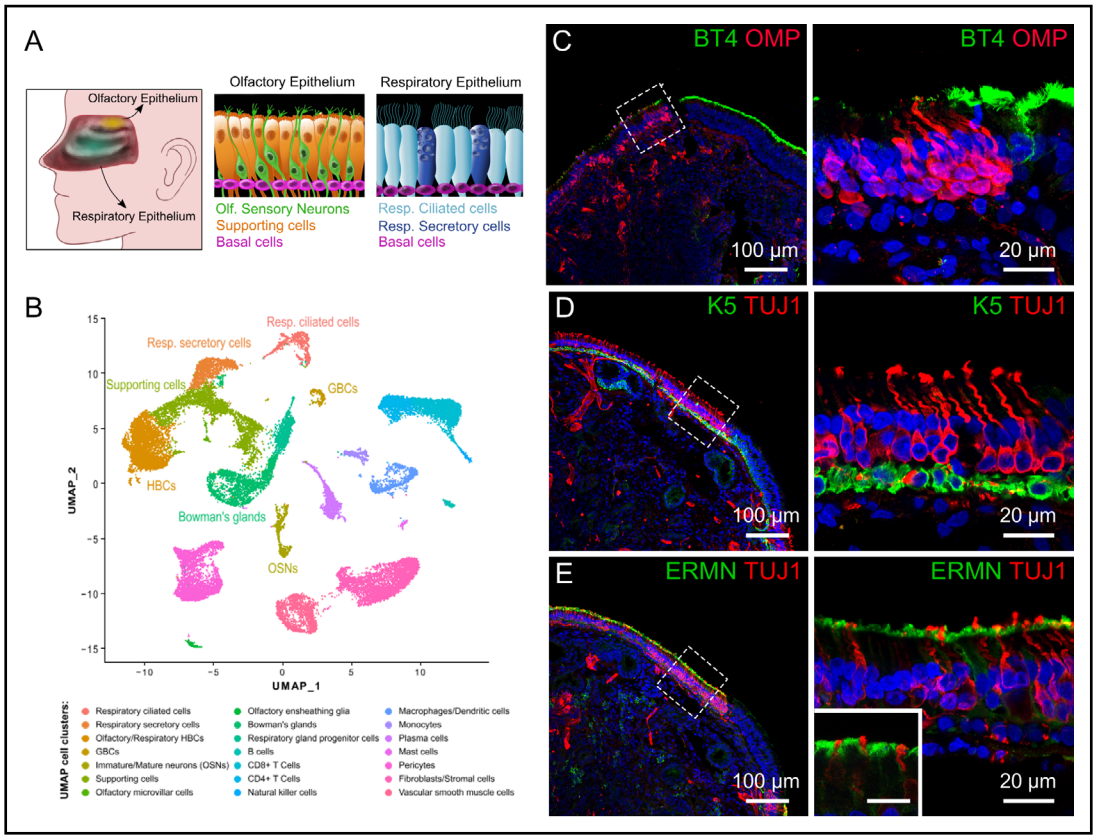


**Fig. 1.** Main cell types in the human olfactory and respiratory epithelium. (A) Schematic representation of the main cell types of the respiratory epithelium and olfactory epithelium. (B) Visualization of the clustering results from the scRNA-seq data produced in Durante et al. [42] on a uniform manifold approximation and projection (UMAP) plot. The cell type annotation of each cluster is noted on the color key legend and labels. (C-E) Confocal images of sections of human nasal epithelium. β-tubulin IV (BT4) is a marker for the cilia of respiratory ciliated cells (green) and OMP for mature olfactory sensory neurons (red) (C). β-tubulin III (TUJ1) is a marker for neurons (red) and Keratin 5 (K5) for basal cells both in the respiratory and olfactory epithelium (green) (D). ERMN is a marker for the apical part of olfactory supporting cells (green) and does not co-localize with the neuronal marker TUJ1 (red) (E). Higher magnification images taken from the dashed squares are shown in the right columns (C-E). At low magnification (left panels in C-E), the transition zone between olfactory and respiratory epithelium is clearly observed. The respiratory epithelium can easily be distinguished by BT4 expression, while the olfactory epithelium is marked by OMP, TUJ1 or ERMN. Inset scale bar in the right panel in (E) is 10 µm. Cell nuclei were stained with DAPI (blue).

by fluorescence immunohistochemistry. In the respiratory epithelium (apically stained by β-tubulin IV), ACE2 was expressed in many respiratory cells including basal cells lying the basal lamina (Fig. 2C). Moreover, as nasal brushing produced many isolated respiratory cells (but not olfactory cells), we performed immunocytochemistry to clearly identify protein localization and found that most isolated ciliated respiratory cells (marked by β-tubulin IV) also expressed ACE2 (Fig. 2D). However, we did not observe co-localization of ACE2 and the ciliary marker β-tubulin IV but a rather basolateral ACE2 expression and mostly mutually exclusive with β-tubulin IV, indicating that ACE2 is not expressed in the apical cilia. Transcriptomic analysis indicates that *ACE2* is also expressed in respiratory secretory cells (Fig. 2A-B), which do not have an apical ciliary tuft. In our immunocytochemistry experiments several cells morphologically resembling secretory cells also expressed ACE2 but we did not further characterize them with specific markers (Fig. 2C).

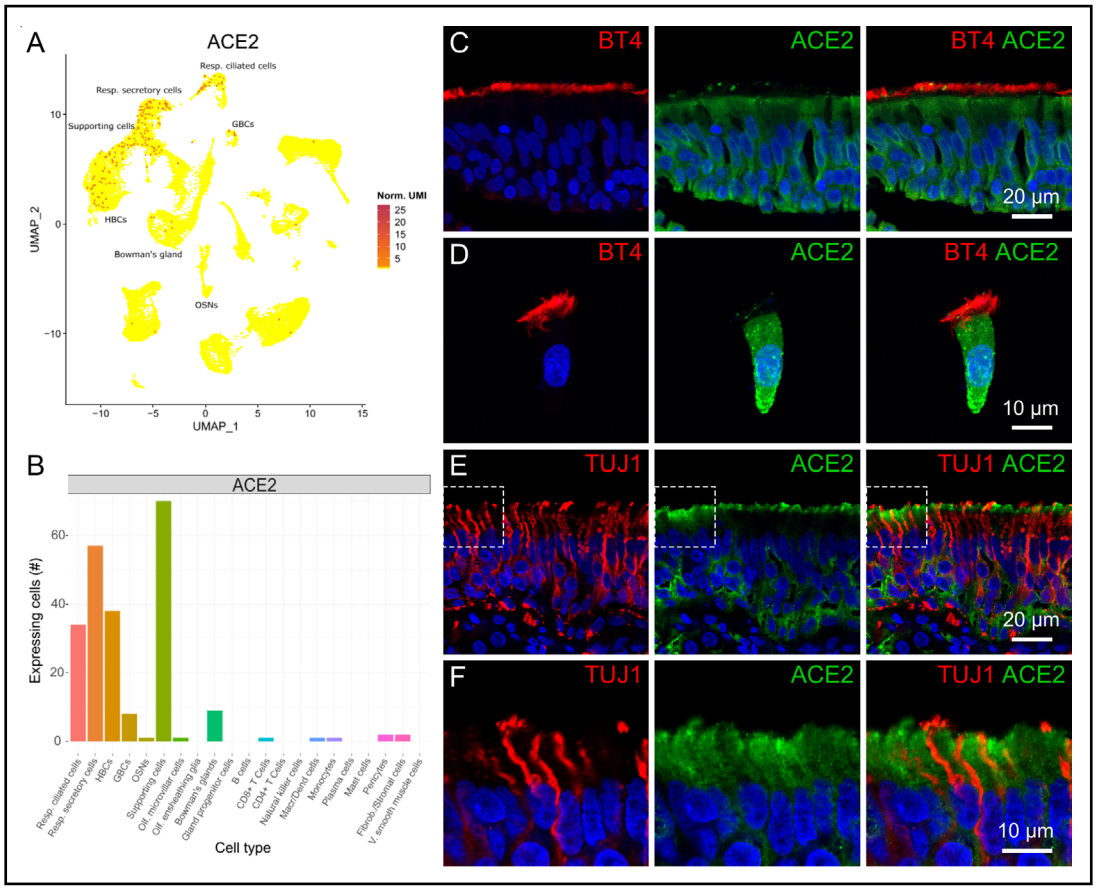


**Fig. 2.** ACE2 transcript and protein expression. (A) Normalized expression levels of *ACE2* shown on the UMAP plot. (B) Bar plot displaying the number of different cell types expressing *ACE2*. (C) Section of human respiratory epithelium immunostained for BT4 (red) and ACE2 (green). (D) A dissociated respiratory ciliated cell immunostained for BT4 (red) and ACE2 (green) showing that ACE2 is highly expressed in the cell except in the cilia. (E-F) Sections of human olfactory epithelium immunostained for TUJ1 (red) and ACE2 (green). Higher magnification images taken from the dashed squares in (E) are shown in (F). ACE2 is expressed in basal and supporting cells but not in neurons (F). Cell nuclei were stained with DAPI (blue).

Fig. 2E and F show that ACE2 staining in the olfactory epithelium was mutually exclusive with TUJ1, resembling the mutually exclusive expression of TUJ1 and ERMN (Fig. 1E), thus validating the transcriptomic results that show expression of *ACE2* in supporting cells and lack of signal in olfactory neurons (Fig. 2A-B). ACE2 was mainly concentrated in the apical half of the supporting cells and it surrounded the TUJ1 positive neuronal dendrites and knobs (Fig. 2E-F). ACE2 was also localized to the basal part of the epithelium indicating that it is also expressed in olfactory basal cells (Fig. 2E, see also Fig. 4C-D).

In summary, we confirmed that ACE2 is expressed both in the human respiratory and olfactory epithelium where it is mainly found in supporting and basal cells but not in neurons.

*TMEM16F transcript and protein expression*

As TMEM16F has been shown to be involved in SARS-CoV-2 Spike-induced syncytia formation in several cells and tissues [20, 35], we investigated the expression of TMEM16F and described for the first time the expression and localization of TMEM16F in the human respiratory and olfactory epithelium.

Transcriptomic analysis indicated that *TMEM16F* is expressed in several cell types of the nasal tissue (Fig. 3A-B), especially in respiratory secretory and ciliated cells and in olfactory supporting cells. Immunohistochemistry confirmed the expression of TMEM16F

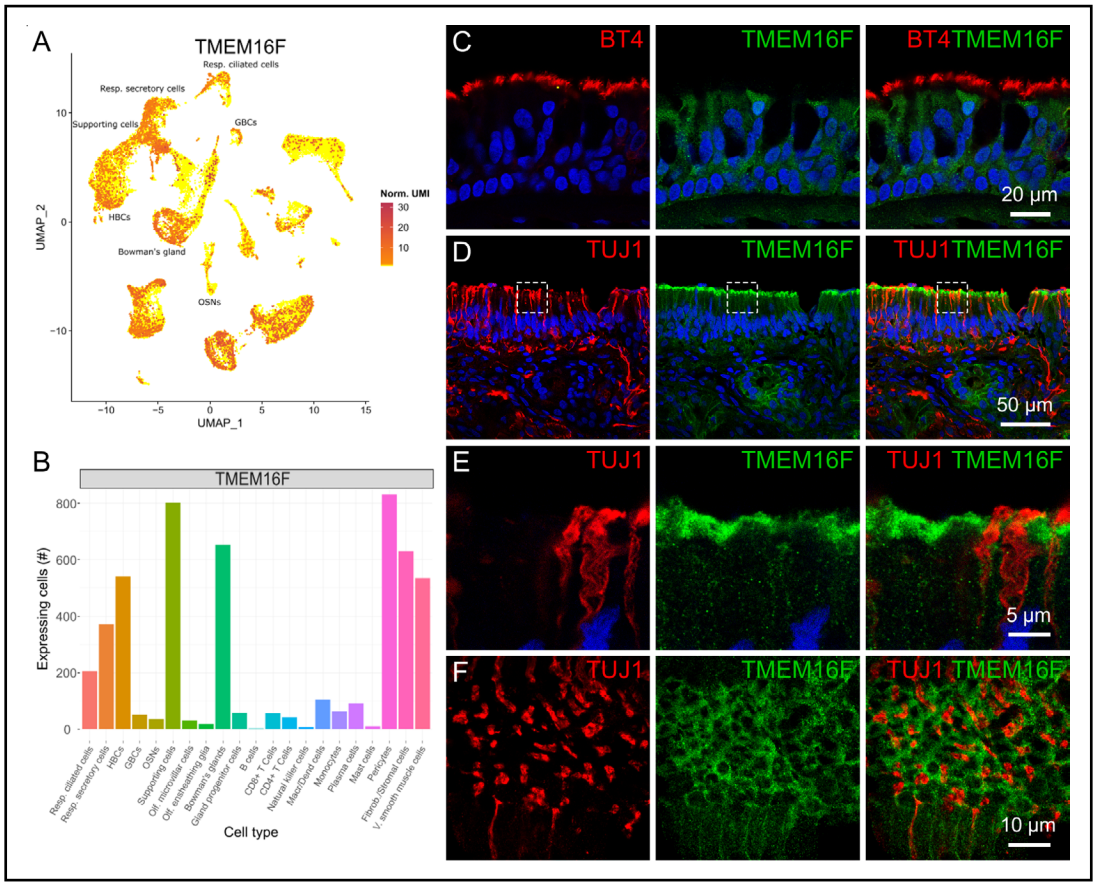


**Fig. 3.** TMEM16F transcript and protein expression. (A) Normalized expression levels of *TMEM16F* shown on the UMAP plot. (B) Bar plot displaying the number of different cell types expressing *TMEM16F*. (C) Section of human respiratory epithelium immunostained for BT4 (red) and TMEM16F (green). TMEM16F shows a faint but consistent expression in most cells of the respiratory epithelium. (D) Section of human olfactory epithelium immunostained for TUJ1 (red) and TMEM16F (green). TMEM16F is highly expressed in the apical region of the olfactory epithelium and in cells of secretory glands. (E) High magnification images of the apical region of the olfactory epithelium taken from the dashed squares in (D). TMEM16F stains the apical region of supporting cells and do not show co-localization with the neuronal marker TUJ1. The staining of TMEM16F at the apical region is similar to ERMN expression pattern shown in Fig. 1E. (F) En-face view of a section of olfactory epithelium stained with TUJ1 (red) and TMEM16F (green). TMEM16F shows no co-localization with the neuronal marker TUJ1. Cell nuclei were stained with DAPI (blue). See also Supplementary Fig. S2.

in several cells of the respiratory epithelium (Fig. 3C). In the olfactory epithelium, we also found staining of TMEM16F with higher intensity at the apical side (Fig. 3D-E). Similarly to ACE2 (Fig. 2E-F), TMEM16F did not co-localize with the neuronal marker TUJ1 indicating the lack of expression in olfactory sensory neurons (Fig. 3D-E). Fig. 3E clearly shows apical dendrite/knob regions of three neurons marked with TUJ1 but not stained for TMEM16F. The expression pattern of TMEM16F resembles that of ERMN that intensely stains the apical portion of supporting cells (Fig. 1E and 3E). We also imaged tangential/oblique sections of the olfactory epithelium to better visualize the intriguing pattern of TMEM16F expression: Fig. 3F shows that round/oval shaped structures marked by TMEM16F (green) surround the knobs of olfactory sensory neurons marked by TUJ1 (red), further showing the expression of TMEM16F in non-neuronal cells. Furthermore, the antibody against TMEM16F marked several glandular cells, most likely belonging to Bowman's glands, beneath the basal lamina of the olfactory epithelium (Fig. 3D and 4C).

In summary, we showed that TMEM16F is expressed both in the human respiratory and olfactory epithelium where it mostly localizes in the apical region of supporting cells with a pattern similar to that of ERMN.

*TMEM16F and ACE2 co-expression in supporting cells of the olfactory epithelium*

To better evaluate the co-expression levels of *ACE2* and *TMEM16F* in different cell types, we plotted the mean expression levels for each cell type (Fig. 4A) and the number of cells expressing both transcripts (Fig. 4B). Olfactory supporting cells, respiratory ciliated and secretory cells showed the highest correlated expression levels for *ACE2* and *TMEM16F*.

Immunohistochemistry experiments on the olfactory epithelium using ACE2 and TMEM16F antibodies showed the co-localization of the two proteins at the apical side of the epithelium. Fig. 4C and D (left panels) clearly confirm ACE2 staining in the upper portion of the olfactory epithelium and in the basal side, similarly to results shown in Fig. 2E obtained with a different antibody. TMEM16F also localized to the apical side of the olfactory epithelium, with some staining more distal than that of ACE2.

All together, these results strengthen the possibility that SARS-CoV-2 Spike protein could bind to ACE2 and produce the activation of TMEM16F in the same cell with subsequent cell-to-cell fusion. It has also been shown that interferon-induced transmembrane proteins inhibit Spike-induced cell-to-cell fusion whereas TMPRSS2 accelerates Spike-mediated syncytia and counteracts the inhibitory effect of the interferon-induced transmembrane proteins [21]. Here, we evaluated the co-expression levels of *TMPRSS2*, *ACE2* and *TMEM16F* in different cell types (Fig. S1A-D) and found that olfactory supporting cells, respiratory ciliated and secretory cells show the highest correlated expression levels for the three genes, indicating that syncytia could be formed also if interferon is released by cells infected by SARS-CoV-2.

In summary, we showed that TMEM16F is co-expressed with ACE2 at the apical part of human olfactory supporting cells and could be contributing to cell-to-cell fusion induced by Spike binding to ACE2. Syncytia formation by supporting cells could cause olfactory dysfunctions.

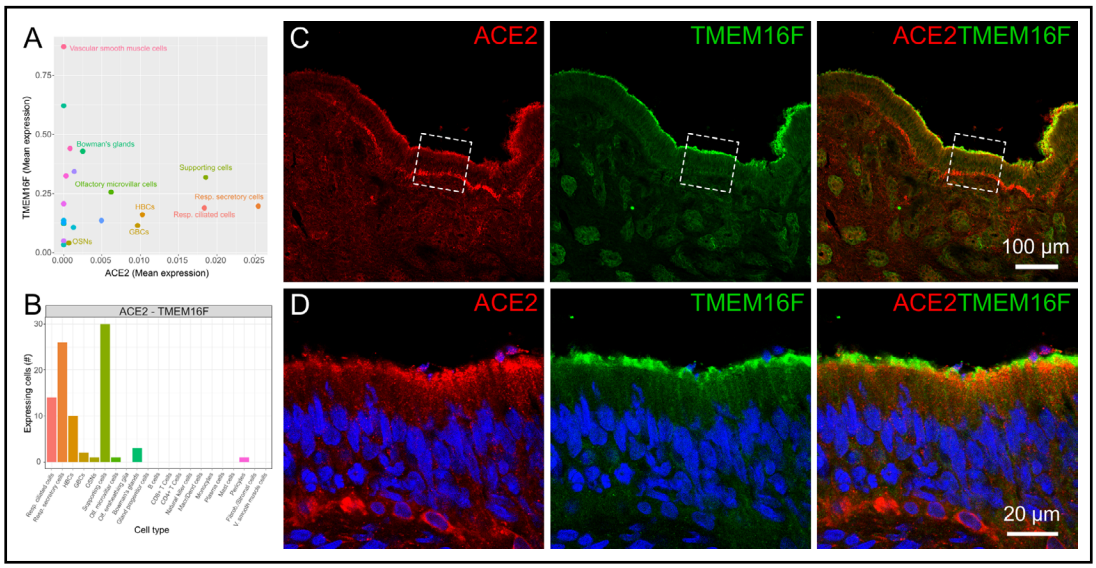


**Fig. 4.** TMEM16F and ACE2 co-expression in supporting cells of the olfactory epithelium. (A) Co-expression of *ACE2* and *TMEM16F* in the different cell clusters. Mean normalized expression levels are plotted. (B) Bar plot displaying the number of cells co-expressing *ACE2* and *TMEM16F* in each cluster. (C) Section of human olfactory epithelium immunostained for ACE2 (red) and TMEM16F (green). ACE2 and TMEM16F are co-expressed in the apical region of supporting cells of the olfactory epithelium. (D) High magnification images of the apical region of the olfactory epithelium taken from the dashed squares in (C). Cell nuclei were stained with DAPI (blue).

## Discussion

It has recently been shown that SARS-CoV-2 pathogenic mechanisms include the formation of syncytia in several cellular models and in tissues biopsies from COVID-19 patients [20, 21, 24, 25, 30, 55]. Some studies have shown that the molecular pathway that leads to syncytia formation after the binding of SARS-CoV-2 Spike to ACE2 involves TMEM16F [20, 35, 56]. As the molecular mechanisms underlying dysfunctions of the sense of smell in COVID-19 are still largely unknown, we sought to set a working hypothesis for SARS-CoV-2 pathogenesis in the olfactory epithelium that includes the possibility of syncytia formation. Our results provide the first demonstration that TMEM16F is co-expressed with ACE2 in the human olfactory epithelium at the apical part of olfactory supporting cells. Thus, the molecular machinery necessary to induce cell fusion upon binding of Spike is present in the supporting cells of the olfactory epithelium and may constitute a possible mechanism damaging the olfactory epithelium and producing dysfunctions in the sense of smell.

TMEM16F is a very intriguing transmembrane protein that functions both as calcium-activated lipid scramblase and ion channel [31–34, 50, 57]. TMEM16F as a scramblase has been shown to promote platelet association and cell-to-cell fusion [20, 50, 58]. The activation of TMEM16F caused by the SARS-CoV-2 Spike protein has been shown to be relevant for COVID-19 pathogenesis. It prompts pro-coagulant activity in platelets via lipid scrambling promoting thrombin formation, thus causing SARS-CoV-2-induced thrombosis [22, 35]. In the alveoli, TMEM16F promotes SARS-CoV-2-Spike mediated syncytia formation by exposing phosphatidylserine on the outer leaflet of plasma membrane [20, 30, 35, 36]. At least two possible mechanisms have been hypothesized for the activation of TMEM16F by Spike [20, 22, 25]: TMEM16F could be directly activated upon binding of Spike to ACE2 in the same cell, or TMEM16F could be activated by an induced increase in intracellular calcium. Activation of the scramblase TMEM16F then causes phosphatidylserine insertion on the outer leaflet of the plasma membrane, which is the signal for cell-to-cell fusion.

Although olfactory impairments are well documented during and post COVID-19 [1–6] the pathophysiological mechanisms are still largely elusive. Contrary to other forms of olfactory dysfunction associated with respiratory viral infections [59], a nasal mucosal oedema obstructing the olfactory cleft and leading to a conductive loss could explain only a small fraction of the cases of smell alteration caused by COVID-19. In fact, nasal obstruction and an altered sense of smell have been observed to be frequently dissociated symptoms also during the acute phase of COVID-19 [9, 60].

Supporting cells are the primary target of SARS-CoV-2 in the olfactory epithelium [43–45, 61–63] and we have shown here that they co-express ACE2 and TMEM16F and could therefore form Spike-induced syncytia that may contribute to a prolonged smell loss. Indeed, although olfactory sensory neurons do not appear to be directly affected by SARS-CoV-2, it is important to note that olfactory supporting cells do not simply surround the dendrites of olfactory sensory neurons but they enwrap the dendrites, especially when neurons become mature, forming a cell-in-cell structure with olfactory sensory neurons [54, 64, 65]. Thus, if supporting cells form syncytia, also the functionality of olfactory sensory neurons is likely to be compromised.

Another possible scenario involves TMEM16F working as a calcium-activated nonselective ion channel. Indeed, we have shown here that TMEM16F is localized in the distal apical part of supporting cells that is in contact with the mucus layer in the nasal cavity. The mucus composition is very important to maintain the ionic gradients involved in transducing odorant binding to the receptor in the cilia of olfactory sensory neurons into action potentials sent to the brain. Thus, if TMEM16F is activated as ion channel, it may modify the mucus ionic composition as it is permeable to various ions, including chloride, calcium and sodium [34, 50, 66–71]. In humans (as well as in mice), the cyclic nucleotide-gated channel A2 (CNGA2) has a crucial role in olfactory signal transduction [72, 73] and a reduction of the inward transduction current carried by calcium and sodium ions through CNG channels of olfactory sensory neurons may decrease the odorant response [74–77]. In

addition, in human olfactory sensory neurons the chloride current via the calcium-activated chloride channel TMEM16B/ANO2 [78, 79] may participate in odorant transduction, and therefore an alteration of the chloride ion gradient that reduces the odorant-induced current, may decrease olfactory neurons sensitivity and ultimately cause smell impairments, as it occurs in mice [79–83].

Although some reports did not find signs of inflammatory response in the olfactory cleft [84, 85], a recent study showed the presence of sustained inflammation in the olfactory epithelium and olfactory bulb [63]. It is known that interferon-induced transmembrane proteins inhibit Spike-induced cell-to-cell fusion but it has also been reported that TMPRSS2 counteracts this inhibitory activity by significantly increasing Spike protein syncytia formation [21, 24, 25]. Thus, human olfactory supporting cells have all the molecular components necessary to promote viral infection, replication and syncytia formation also in the presence of inflammation. In addition, several transcriptomic signatures implicate T-cell recruitment [63], but it has been shown that Spike-mediated syncytia can also internalize various T-cell lines causing their death by deterioration of their plasma membrane [25, 30].

To our knowledge, syncytia were overlooked in the few published reports about respiratory and olfactory epithelium in COVID-19 patients and therefore, at present, there is no evidence of syncytia formation in nasal epithelia. However, the presence of syncytia has been demonstrated in air-liquid interphase cultures of cells brushed from the nose and infected with SARS-CoV-2 (Fig. 1 of Capraro et al. [86]). In agreement with previous studies indicating that the nasal respiratory epithelium is one of the primary targets of SARS-CoV-2 [87, 88], we found that ACE2 is expressed in respiratory cells. In addition, we showed that both TMEM16F and ACE2 are expressed in the respiratory epithelium, where they may promote cell-to-cell fusion. It should also be considered, though, that syncytia in various tissues were observed only in the severe stages of the disease in COVID-19 patients and may not be present in mild cases [20, 89].

## Conclusion

Our results provide the first evidence that TMEM16F and ACE2 are co-expressed in human olfactory supporting cells and indicate that the loss of smell in COVID-19 may be due also to syncytia formation. TMEM16F is a target for commercially available drugs, such as niclosamide [20, 90], and some lipid-targeting drugs disrupt Spike-mediated membrane fusion [17]. Thus, it may be worth pursuing the possibility to target some of these drugs directly to the nasal epithelia to at least mitigate the olfactory impairments experienced during COVID-19.

## Acknowledgements

We thank Dr. Lily Jan (UCSF) for providing the antibody against TMEM16F.

*Author Contributions*

A.H.C, K.G.V. performed immunohistochemistry and confocal microscopy with the help of G.G.. P.B.R., M.T., N.G. and G.T. collected human biopsies. U.R. and R.S performed scRNA-seq data analysis. A.M., M.D. and A.H.C. conceptualized the project and designed experiments. M.D. and A.M. wrote the manuscript with comments from all the other authors.

*Funding*

This work was funded by the Italian Ministry of Education, University and Research 2010599KBR (A.M.).

*Statement of Ethics*

Subjects have given their written informed consent and the study protocol has been approved by the Ethics Committee on Clinical Investigation of the University of Trieste (nr 232/2016 and 110/2021).

## Disclosure Statement

The authors declare they have no conflicts of interest.

## References

1 Boscolo-Rizzo P, Menegaldo A, Fabbris C, Spinato G, Borsetto D, Vaira LA, Calvanese L, Pettorelli A, Sonego M, Frezza D, Bertolin A, Cestaro W, Rigoli R, D'Alessandro A, Tirelli G, Da Mosto MC, Menini A, Polesel J, Hopkins C: Six-Month Psychophysical Evaluation of Olfactory Dysfunction in Patients with COVID-19. Chem Senses 2021;46:bjab006.

2 Cecchetto C, Di Pizio A, Genovese F, Calcinoni O, Macchi A, Dunkel A, Ohla K, Spinelli S, Farruggia MC, Joseph PV, Menini A, Cantone E, Dinnella C, Cecchini MP, D'Errico A, Mucignat-Caretta C, Parma V, Dibattista M: Assessing the extent and timing of chemosensory impairments during COVID-19 pandemic. Sci Rep 2021;11:17504.

3 Giacomelli A, Pezzati L, Conti F, Bernacchia D, Siano M, Oreni L, Rusconi S, Gervasoni C, Ridolfo AL, Rizzardini G, Antinori S, Galli M: Self-reported Olfactory and Taste Disorders in Patients With Severe Acute Respiratory Coronavirus 2 Infection: A Cross-sectional Study. Clin Infect Dis Off Publ Infect Dis Soc Am 2020;71:889–890.

4 Iannuzzi L, Salzo AE, Angarano G, Palmieri VO, Portincasa P, Saracino A, Gelardi M, Dibattista M, Quaranta N: Gaining Back What Is Lost: Recovering the Sense of Smell in Mild to Moderate Patients After COVID-19. Chem Senses 2020;45:875–881.

5 Parma V, Ohla K, Veldhuizen MG, Niv MY, Kelly CE, Bakke AJ, Cooper KW, Bouysset C, Pirastu N, Dibattista M, Kaur R, Liuzza MT, Pepino MY, Schöpf V, Pereda-Loth V, Olsson SB, Gerkin RC, Rohlfs Domínguez P, Albayay J, Farruggia MC, et al.: More Than Smell—COVID-19 Is Associated With Severe Impairment of Smell, Taste, and Chemesthesis. Chem Senses 2020;45:609–622.

6 Spinato G, Fabbris C, Polesel J, Cazzador D, Borsetto D, Hopkins C, Boscolo-Rizzo P: Alterations in Smell or Taste in Mildly Symptomatic Outpatients With SARS-CoV-2 Infection. JAMA 2020;323:2089–2090.

7 Cavazzana A, Larsson M, Münch M, Hähner A, Hummel T: Postinfectious olfactory loss: A retrospective study on 791 patients. Laryngoscope 2018;128:10–15.

8 Temmel AFP, Quint C, Schickinger-Fischer B, Klimek L, Stoller E, Hummel T: Characteristics of Olfactory Disorders in Relation to Major Causes of Olfactory Loss. Arch Otolaryngol Neck Surg 2002;128:635–641.

9 Boscolo-Rizzo P, Borsetto D, Fabbris C, Spinato G, Frezza D, Menegaldo A, Mularoni F, Gaudioso P, Cazzador D, Marciani S, Frasconi S, Ferraro M, Berro C, Varago C, Nicolai P, Tirelli G, Da Mosto MC, Obholzer R, Rigoli R, Polesel J, et al.: Evolution of Altered Sense of Smell or Taste in Patients With Mildly Symptomatic COVID-19. JAMA Otolaryngol Neck Surg 2020;146:729–732.

10 Gerkin RC, Ohla K, Veldhuizen MG, Joseph PV, Kelly CE, Bakke AJ, Steele KE, Farruggia MC, Pellegrino R, Pepino MY, Bouysset C, Soler GM, Pereda-Loth V, Dibattista M, Cooper KW, Croijmans I, Di Pizio A, Ozdener MH, Fjaeldstad AW, Lin C, et al.: Recent Smell Loss Is the Best Predictor of COVID-19 Among Individuals With Recent Respiratory Symptoms. Chem Senses 2021;46:bjaa081.

11 Menni C, Valdes AM, Freidin MB, Sudre CH, Nguyen LH, Drew DA, Ganesh S, Varsavsky T, Cardoso MJ, El-Sayed Moustafa JS, Visconti A, Hysi P, Bowyer RCE, Mangino M, Falchi M, Wolf J, Ourselin S, Chan AT, Steves CJ, Spector TD: Real-time tracking of self-reported symptoms to predict potential COVID-19. Nat Med 2020;26:1037–1040.

12 Wu F, Zhao S, Yu B, Chen YM, Wang W, Song ZG, Hu Y, Tao ZW, Tian JH, Pei YY, Yuan ML, Zhang YL, Dai FH, Liu Y, Wang QM, Zheng JJ, Xu L, Holmes EC, Zhang YZ: A new coronavirus associated with human respiratory disease in China. Nature 2020;579:265–269.

13 Tyrrell DAJ, Almeida JD, Cunningham CH, Dowdle WR, Hofstad MS, McIntosh K, Tajima M, Zakstelskaya LY, Easterday BC, Kapikian A, Bingham RW: Coronaviridae 1. Intervirology 1975;5:76–82.
14 Hoffmann M, Kleine-Weber H, Schroeder S, Krüger N, Herrler T, Erichsen S, Schiergens TS, Herrler G, Wu NH, Nitsche A, Müller MA, Drosten C, Pöhlmann S: SARS-CoV-2 Cell Entry Depends on ACE2 and TMPRSS2 and Is Blocked by a Clinically Proven Protease Inhibitor. Cell 2020;181:271-280.e8.
15 Mittal A, Manjunath K, Ranjan RK, Kaushik S, Kumar S, Verma V: COVID-19 pandemic: Insights into structure, function, and hACE2 receptor recognition by SARS-CoV-2. PLOS Pathog 2020;16:e1008762.
16 Lan J, Ge J, Yu J, Shan S, Zhou H, Fan S, Zhang Q, Shi X, Wang Q, Zhang L, Wang X. Structure of the SARS-CoV-2 spike receptor-binding domain bound to the ACE2 receptor. Nature 2020;581:215–220.
17 Sanders DW, Jumper CC, Ackerman PJ, Bracha D, Donlic A, Kim H, Kenney D, Castello-Serrano I, Suzuki S, Tamura T, Tavares AH, Saeed M, Holehouse AS, Ploss A, Levental I, Douam F, Padera RF, Levy BD, Brangwynne CP: SARS-CoV-2 requires cholesterol for viral entry and pathological syncytia formation. Elife 2021;10:e65962.
18 Hoffmann M, Kleine-Weber H, Pöhlmann S: A Multibasic Cleavage Site in the Spike Protein of SARS-CoV-2 Is Essential for Infection of Human Lung Cells. Mol Cell 2020;78:779-784.e5.
19 Peacock TP, Goldhill DH, Zhou J, Baillon L, Frise R, Swann OC, Kugathasan R, Penn R, Brown JC, Sanchez-David RY, Braga L, Williamson MK, Hassard JA, Staller E, Hanley B, Osborn M, Giacca M, Davidson AD, Matthews DA, Barclay WS: The furin cleavage site in the SARS-CoV-2 spike protein is required for transmission in ferrets. Nat Microbiol 2021;6:899–909.
20 Braga L, Ali H, Secco I, Chiavacci E, Neves G, Goldhill D, Penn R, Jimenez-Guardeño JM, Ortega-Prieto AM, Bussani R, Cannatà A, Rizzari G, Collesi C, Schneider E, Arosio D, Shah AM, Barclay WS, Malim MH, Burrone J, Giacca M: Drugs that inhibit TMEM16 proteins block SARS-CoV-2 spike-induced syncytia. Nature 2021;594:88–93.
21 Buchrieser J, Dufloo J, Hubert M, Monel B, Planas D, Rajah MM, Planchais C, Porrot F, Guivel-Benhassine F, Van der Werf S, Casartelli N, Mouquet H, Bruel T, Schwartz O: Syncytia formation by SARS-CoV-2-infected cells. EMBO J 2020;39:e106267.
22 Cappelletto A, Allan HE, Crescente M, Schneider E, Bussani R, Ali H, Secco I, Vodret S, Simeone R, Mascaretti L, Zacchigna S, Warner TD, Giacca M: SARS-CoV-2 Spike protein activates TMEM16F-mediated platelet pro-coagulant activity. BioRxiv 2021; DOI: 2021.12.14.472668.
23 Lazebnik Y: Cell fusion as a link between the SARS-CoV-2 spike protein, COVID-19 complications, and vaccine side effects. Oncotarget 2021;12:2476–2488.
24 Navaratnarajah CK, Pease DR, Halfmann PJ, Taye B, Barkhymer A, Howell KG, Charlesworth JE, Christensen TA, Kawaoka Y, Cattaneo R, Schneider JW: Highly Efficient SARS-CoV-2 Infection of Human Cardiomyocytes: Spike Protein-Mediated Cell Fusion and Its Inhibition. J Virol 2021;95:e01368-21.
25 Rajah MM, Bernier A, Buchrieser J, Schwartz O: The Mechanism and Consequences of SARS-CoV-2 Spike-Mediated Fusion and Syncytia Formation. J Mol Biol 2021;434:167280.
26 Theuerkauf SA, Michels A, Riechert V, Maier TJ, Flory E, Cichutek K, Buchholz CJ: Quantitative assays reveal cell fusion at minimal levels of SARS-CoV-2 spike protein and fusion from without. iScience 2021;24:102170.
27 Zhu N, Wang W, Liu Z, Liang C, Wang W, Ye F, Huang B, Zhao L, Wang H, Zhou W, Deng Y, Mao L, Su C, Qiang G, Jiang T, Zhao J, Wu G, Song J, Tan W: Morphogenesis and cytopathic effect of SARS-CoV-2 infection in human airway epithelial cells. Nat Commun 2020;11:3910.
28 Murae M, Shimizu Y, Yamamoto Y, Kobayashi A, Houri M, Inoue T, Irie T, Gemba R, Kondo Y, Nakano Y, Miyazaki S, Yamada D, Saitoh A, Ishii I, Onodera T, Takahashi Y, Wakita T, Fukasawa M, Noguchi K: The function of SARS-CoV-2 spike protein is impaired by disulfide-bond disruption with mutation at cysteine-488 and by thiol-reactive N-acetyl-cysteine and glutathione. Biochem Biophys Res Commun 2022;597:30–36.
29 Bryce C, Grimes Z, Pujadas E, Ahuja S, Beasley MB, Albrecht R, Hernandez T, Stock A, Zhao Z, AlRasheed MR, Chen J, Li L, Wang D, Corben A, Haines GK, Westra WH, Umphlett M, Gordon RE, Reidy J, Petersen B, et al.: Pathophysiology of SARS-CoV-2: the Mount Sinai COVID-19 autopsy experience. Mod Pathol 2021;34:1456–1467.
30 Zhang Z, Zheng Y, Niu Z, Zhang B, Wang C, Yao X, Peng H, Franca DN, Wang Y, Zhu Y, Su Y, Tang M, Jiang X, Ren H, He M, Wang Y, Gao L, Zhao P, Shi H, Chen Z, et al.: SARS-CoV-2 spike protein dictates syncytium-mediated lymphocyte elimination. Cell Death Differ 2021;28:2765–2777.

31 Feng S, Dang S, Han TW, Ye W, Jin P, Cheng T, Li J, Jan YN, Jan LY, Cheng Y: Cryo-EM Studies of TMEM16F Calcium-Activated Ion Channel Suggest Features Important for Lipid Scrambling. Cell Rep 2019;28:567-579.
32 Kalienkova V, Clerico Mosina V, Paulino C: The Groovy TMEM16 Family: Molecular Mechanisms of Lipid Scrambling and Ion Conduction. J Mol Biol 2021;433:166941.
33 Picollo A, Malvezzi M, Accardi A: TMEM16 proteins: unknown structure and confusing functions. J Mol Biol 2015;427:94–105.
34 Stabilini S, Menini A, Pifferi S: Anion and Cation Permeability of the Mouse TMEM16F Calcium-Activated Channel. Int J Mol Sci 2021;22:8578.
35 Rajah MM, Hubert M, Bishop E, Saunders N, Robinot R, Grzelak L, Planas D, Dufloo J, Gellenoncourt S, Bongers A, Zivaljic M, Planchais C, Guivel-Benhassine F, Porrot F, Mouquet H, Chakrabarti LA, Buchrieser J, Schwartz O: SARS-CoV-2 Alpha, Beta, and Delta variants display enhanced Spike-mediated syncytia formation. EMBO J 2021;40:e108944.
36 Zaitseva E, Zaitsev E, Melikov K, Arakelyan A, Marin M, Villasmil R, Margolis LB, Melikyan GB, Chernomordik LV: Fusion Stage of HIV-1 Entry Depends on Virus-Induced Cell Surface Exposure of Phosphatidylserine. Cell Host Microbe 2017;22:99-110.e7.
37 Andres KH: The fine structure of the olfactory region of macrosmatic animals. Z Zellforsch Mikrosk Anat 1966;69:140–154.
38 Dibattista M, Pifferi S, Menini A, Reisert J: Alzheimer's Disease: What Can We Learn From the Peripheral Olfactory System? Front Neurosci 2020;14:440.
39 Graziadei PP, Graziadei GA: Neurogenesis and neuron regeneration in the olfactory system of mammals. I. Morphological aspects of differentiation and structural organization of the olfactory sensory neurons. J Neurocytol 1979;8:1–18.
40 Huard JM, Schwob JE: Cell cycle of globose basal cells in rat olfactory epithelium. Dev Dyn 1995;203:17–26.
41 Schwob JE, Jang W, Holbrook EH, Lin B, Herrick DB, Peterson JN, Hewitt Coleman J: Stem and progenitor cells of the mammalian olfactory epithelium: Taking poietic license: Stem and progenitor cells of the Mammalian OE. J Comp Neurol 2017;525:1034–1054.
42 Durante MA, Kurtenbach S, Sargi ZB, Harbour JW, Choi R, Kurtenbach S, Goss GM, Matsunami H, Goldstein BJ: Single-cell analysis of olfactory neurogenesis and differentiation in adult humans. Nat Neurosci 2020;23:323–326.
43 Brann DH, Tsukahara T, Weinreb C, Lipovsek M, Koen Van den Berge, Gong B, Chance R, Macaulay IC, Chou HJ, Fletcher RB, Das D, Street K, Roux de Bezieux H, Choi YG, Risso D, Dudoit S, Purdom E, Mill J, Hachem RA, Matsunami H, et al.: Non-neuronal expression of SARS-CoV-2 entry genes in the olfactory system suggests mechanisms underlying COVID-19-associated anosmia. Sci Adv 2020;6:eabc5801.
44 Fodoulian L, Tuberosa J, Rossier D, Boillat M, Kan C, Pauli V, Egervari K, Lobrinus JA, Landis BN, Carleton A, Rodriguez I: SARS-CoV-2 Receptors and Entry Genes Are Expressed in the Human Olfactory Neuroepithelium and Brain. iScience 2020;23:101839.
45 Khan M, Yoo SJ, Clijsters M, Backaert W, Vanstapel A, Speleman K, Lietaer C, Choi S, Hether TD, Marcelis L, Nam A, Pan L, Reeves JW, Bulck PV, Zhou H, Bourgeois M, Debaveye Y, Munter PD, Gunst J, Jorissen M, et al.: Visualizing in deceased COVID-19 patients how SARS-CoV-2 attacks the respiratory and olfactory mucosae but spares the olfactory bulb. Cell 2021;184:5932-5949.e15.
46 Butler A, Hoffman P, Smibert P, Papalexi E, Satija R: Integrating single-cell transcriptomic data across different conditions, technologies, and species. Nat Biotechnol 2018;36:411–420.
47 Satija R, Farrell JA, Gennert D, Schier AF, Regev A: Spatial reconstruction of single-cell gene expression data. Nat Biotechnol 2015;33:495–502.
48 Stuart T, Butler A, Hoffman P, Hafemeister C, Papalexi E, Mauck WM, Hao Y, Stoeckius M, Smibert P, Satija R: Comprehensive Integration of Single-Cell Data. Cell 2019;177:1888-1902.e21.
49 Scudieri P, Musante I, Venturini A, Guidone D, Genovese M, Cresta F, Caci E, Palleschi A, Poeta M, Santamaria F, Ciciriello F, Lucidi V, Galietta LJV: Ionocytes and CFTR Chloride Channel Expression in Normal and Cystic Fibrosis Nasal and Bronchial Epithelial Cells. Cells 2020;9:2090.
50 Yang H, Kim A, David T, Palmer D, Jin T, Tien J, Huang F, Cheng T, Coughlin SR, Jan YN, Jan LY: TMEM16F Forms a Ca2+-Activated Cation Channel Required for Lipid Scrambling in Platelets during Blood Coagulation. Cell 2012;151:111–122.

51 Aigouy B, Mirouse V: ScientiFig: a tool to build publication-ready scientific figures. Nat Methods 2013;10:1048.
52 Holbrook EH, Wu E, Curry WT, Lin DT, Schwob JE: Immunohistochemical characterization of human olfactory tissue. Laryngoscope 2011;121:1687–1701.
53 Hahn CG, Han LY, Rawson NE, Mirza N, Borgmann-Winter K, Lenox RH, Arnold SE: In vivo and in vitro neurogenesis in human olfactory epithelium. J Comp Neurol 2005;483:154–163.
54 Liang F: Olfactory receptor neuronal dendrites become mostly intra-sustentacularly enwrapped upon maturity. J Anat 2018;232:674–685.
55 Bussani R, Schneider E, Zentilin L, Collesi C, Ali H, Braga L, Volpe MC, Colliva A, Zanconati F, Berlot G, Silvestri F, Zacchigna S, Giacca M: Persistence of viral RNA, pneumocyte syncytia and thrombosis are hallmarks of advanced COVID-19 pathology. EBioMedicine 2020;61:103104.
56 Lin L, Li Q, Wang Y, Shi Y: Syncytia formation during SARS-CoV-2 lung infection: a disastrous unity to eliminate lymphocytes. Cell Death Differ 2021;28:2019–2021.
57 Suzuki J, Umeda M, Sims PJ, Nagata S: Calcium-dependent phospholipid scrambling by TMEM16F. Nature 2010;468:834–838.
58 Baig AA, Haining EJ, Geuss E, Beck S, Swieringa F, Wanitchakool P, Schuhmann MK, Stegner D, Kunzelmann K, Kleinschnitz C, Heemskerk JWM, Braun A, Nieswandt B: TMEM16F-Mediated Platelet Membrane Phospholipid Scrambling Is Critical for Hemostasis and Thrombosis but not Thromboinflammation in Mice—Brief Report. Arterioscler Thromb Vasc Biol 2016;36:2152–2157.
59 Hummel T, Rothbauer C, Barz S, Grosser K, Pauli E, Kobald G: Olfactory Function in Acute Rhinitisa. Ann N Y Acad Sci 1998;855:616–624.
60 Lechien JR, Chiesa-Estomba CM, De Siati DR, Horoi M, Le Bon SD, Rodriguez A, Dequanter D, Blecic S, El Afia F, Distinguin L, Chekkoury-Idrissi Y, Hans S, Delgado IL, Calvo-Henriquez C, Lavigne P, Falanga C, Barillari MR, Cammaroto G, Khalife M, Leich P, et al.: Olfactory and gustatory dysfunctions as a clinical presentation of mild-to-moderate forms of the coronavirus disease (COVID-19): a multicenter European study. Eur Arch Otorhinolaryngol 2020;277:2251–2261.
61 Baig AM, Khaleeq A, Ali U, Syeda H: Evidence of the COVID-19 virus targeting the CNS: tissue distribution, host–virus interaction, and proposed neurotropic mechanisms. ACS Chem Neurosci 2020;11:995-998.
62 Cooper KW, Brann DH, Farruggia MC, Bhutani S, Pellegrino R, Tsukahara T, Weinreb C, Joseph PV, Larson ED, Parma V, Albers MW, Barlow LA, Datta SR, Pizio AD: COVID-19 and the Chemical Senses: Supporting Players Take Center Stage. Neuron 2020;107:219–233.
63 Frere JJ, Serafini RA, Pryce KD, Zazhytska M, Oishi K, Golynker I, Panis M, Zimering J, Horiuchi S, Hoagland DA, Møller R, Ruiz A, Overdevest JB, Kodra A, Canoll PD, Goldman JE, Borczuk AC, Chandar V, Bram Y, Schwartz R, et al.: SARS-CoV-2 infection results in lasting and systemic perturbations post recovery. BioRxiv 2022; DOI: 10.1101/2022.01.18.476786.
64 Morrison EE, Costanzo RM: Morphology of olfactory epithelium in humans and other vertebrates. Microsc Res Tech 1992;23:49–61.
65 Liang F: Sustentacular Cell Enwrapment of Olfactory Receptor Neuronal Dendrites: An Update. Genes 2020;11:493.
66 Grubb S, Poulsen KA, Juul CA, Kyed T, Klausen TK, Larsen EH, Hoffmann EK: TMEM16F (Anoctamin 6), an anion channel of delayed Ca2+ activation. J Gen Physiol 2013;141:585–600.
67 Henkel B, Drose DR, Ackels T, Oberland S, Spehr M, Neuhaus EM: Co-expression of Anoctamins in Cilia of Olfactory Sensory Neurons. Chem Senses 2015;40:73–87.
68 Ousingsawat J, Wanitchakool P, Kmit A, Romao AM, Jantarajit W, Schreiber R, Kunzelmann K: Anoctamin 6 mediates effects essential for innate immunity downstream of P2X7 receptors in macrophages. Nat Commun 2015;6:6245.
69 Shimizu T, Iehara T, Sato K, Fujii T, Sakai H, Okada Y: TMEM16F is a component of a Ca2+-activated Cl− channel but not a volume-sensitive outwardly rectifying Cl− channel. Am J Physiol-Cell Physiol 2013;304:C748–C759.
70 Ye W, Han TW, He M, Jan YN, Jan LY: Dynamic change of electrostatic field in TMEM16F permeation pathway shifts its ion selectivity. Elife 2019;8:e45187.
71 Yu K, Whitlock JM, Lee K, Ortlund EA, Yuan Cui Y, Hartzell HC: Identification of a lipid scrambling domain in ANO6/TMEM16F. Elife 2015;4:e06901.

72 Karstensen H g., Mang Y, Fark T, Hummel T, Tommerup N: The first mutation in CNGA2 in two brothers with anosmia. Clin Genet 2015;88:293–296.
73 Sailani MR, Jingga I, MirMazlomi SH, Bitarafan F, Bernstein JA, Snyder MP, Garshasbi M: Isolated Congenital Anosmia and CNGA2 Mutation. Sci Rep 2017;7:2667.
74 Kleene SJ: The Electrochemical Basis of Odor Transduction in Vertebrate Olfactory Cilia. Chem Senses 2008;33:839–859.
75 Boccaccio A, Menini A, Pifferi S: The cyclic AMP signaling pathway in the rodent main olfactory system. Cell Tissue Res 2021;383:429–443.
76 Pifferi S, Boccaccio A, Menini A: Cyclic nucleotide-gated ion channels in sensory transduction. FEBS Lett 2006;580:2853–2859.
77 Dibattista M, Amjad A, Maurya DK, Sagheddu C, Montani G, Tirindelli R, Menini A: Calcium-activated chloride channels in the apical region of mouse vomeronasal sensory neurons. J Gen Physiol 2012;140:3–15.
78 Olender T, Keydar I, Pinto JM, Tatarskyy P, Alkelai A, Chien MS, Fishilevich S, Restrepo D, Matsunami H, Gilad Y, Lancet D: The human olfactory transcriptome. BMC Genomics 2016;17:619.
79 Stephan AB, Shum EY, Hirsh S, Cygnar KD, Reisert J, Zhao H: ANO2 is the cilial calcium-activated chloride channel that may mediate olfactory amplification. Proc Natl Acad Sci 2009;106:11776–11781.
80 Dibattista M, Pifferi S, Boccaccio A, Menini A, Reisert J: The long tale of the calcium activated Cl- channels in olfactory transduction. Channels (Austin) 2017;11:399-414.
81 Neureither F, Stowasser N, Frings S, Möhrlen F: Tracking of unfamiliar odors is facilitated by signal amplification through anoctamin 2 chloride channels in mouse olfactory receptor neurons. Physiol Rep 2017;5:e13373.
82 Pietra G, Dibattista M, Menini A, Reisert J, Boccaccio A: The Ca2+-activated Cl– channel TMEM16B regulates action potential firing and axonal targeting in olfactory sensory neurons. J Gen Physiol 2016;148:293–311.
83 Zak JD, Grimaud J, Li RC, Lin CC, Murthy VN: Calcium-activated chloride channels clamp odor-evoked spike activity in olfactory receptor neurons. Sci Rep 2018;8:10600.
84 Galougahi MK, Ghorbani J, Bakhshayeshkaram M, Naeini AS, Haseli S: Olfactory Bulb Magnetic Resonance Imaging in SARS-CoV-2-Induced Anosmia: The First Report. Acad Radiol 2020;27:892–893.
85 Vaira LA, Hopkins C, Sandison A, Manca A, Machouchas N, Turilli D, Lechien JR, Barillari MR, Salzano G, Cossu A, Saussez S, Riu GD: Olfactory epithelium histopathological findings in long-term coronavirus disease 2019 related anosmia. J Laryngol Otol 2020;134:1123–1127.
86 Capraro A, Wong SL, Adhikari A, Allan KM, Patel HR, Zhong L, Raftery M, Jaffe A, Yeang M, Aggarwal A, Wu L, Pandzic E, Whan RM, Turville S, Vittorio O, Bull RA, Kaakoush N, Rawlinson WD, Tedla N, Vafaee F, et al.: Ageing impairs the airway epithelium defence response to SARS-CoV-2. BioRxiv 2021; DOI: 2021.04.05.437453.
87 Chen G, Wu D, Guo W, Cao Y, Huang D, Wang H, Wang T, Zhang X, Chen H, Yu H, Zhang X, Zhang M, Wu S, Song J, Chen T, Han M, Li S, Luo X, Zhao J, Ning Q: Clinical and immunological features of severe and moderate coronavirus disease 2019. J Clin Invest 2020;130:2620-2629.
88 Sungnak W, Huang N, Bécavin C, Berg M, Queen R, Litvinukova M, Talavera-López C, Maatz H, Reichart D, Sampaziotis F, others: SARS-CoV-2 entry factors are highly expressed in nasal epithelial cells together with innate immune genes. Nat Med 2020;26:681-687.
89 Koch J, Uckeley ZM, Lozach P: SARS-CoV-2 variants as super cell fusers: cause or consequence of COVID-19 severity? EMBO J 2021;40:e110041.
90 Cheng Y, Feng S, Puchades C, Ko J, Figueroa E, Chen Y, Wu H, Gu S, Han T, Li J, Ho B, Shoichet B, Jan YN, Jan L: Identification of a conserved drug binding pocket in TMEM16 proteins [Preprint]. Res Sq 2022; DOI: 10.21203/rs.3.rs-1296933/v1.